

What Fermilab $(g-2)_\mu$ experiment tells us about discovering SUSY at HL-LHC and HE-LHC

Amin Aboubrahim,^{1,*} Michael Klasen,^{1,†} and Pran Nath^{2,‡}

¹*Institut für Theoretische Physik, Westfälische Wilhelms-Universität Münster,
Wilhelm-Klemm-Straße 9, 48149 Münster, Germany*

²*Department of Physics, Northeastern University, Boston, MA 02115-5000, USA*

(Dated: October 14, 2021)

Using an artificial neural network we explore the parameter space of supergravity grand unified models consistent with the combined Fermilab E989 and Brookhaven E821 data on $(g-2)_\mu$. The analysis indicates that the region favored by the data is the one generated by gluino-driven radiative breaking of the electroweak symmetry. This region naturally leads to a split sparticle spectrum with light sleptons and weakinos but heavy squarks, with the stau and the chargino as the lightest charged particles. We show that if the entire deviation from the standard model $(g-2)_\mu$ arises from supersymmetry, then supersymmetry is discoverable at HL-LHC and HE-LHC via production and decay of sleptons within the optimal integrated luminosity of HL-LHC and with a smaller integrated luminosity at HE-LHC.

PACS numbers:

Introduction: Recently the Fermilab E989 experiment has measured $a_\mu = (g-2)_\mu/2$ with an unprecedented accuracy so that [1]

$$a_\mu^{\text{exp}} = 116592040(54) \times 10^{-11} \quad (\text{Fermilab E989}). \quad (1)$$

This is to be compared with the previous Brookhaven experiment E821 [2, 3] which gave

$$a_\mu^{\text{exp}} = 116592091(63) \times 10^{-11} \quad (\text{Brookhaven E821}). \quad (2)$$

The combined Fermilab and Brookhaven data give

$$a_\mu^{\text{exp}} = 116592061(41) \times 10^{-11} \quad (\text{Combined E989+E821}). \quad (3)$$

The combined result is to be compared with the Standard Model (SM) prediction which gives [4]

$$a_\mu^{\text{SM}} = 116591810(43) \times 10^{-11}, \quad (4)$$

where the Standard Model prediction contains precise quantum electrodynamic, electroweak, hadronic vacuum polarization and hadronic light-by-light contributions. Thus the difference between the combined Fermilab and Brookhaven (FB) result and the SM result is

$$\Delta a_\mu^{\text{FB}} = a_\mu^{\text{exp}} - a_\mu^{\text{SM}} = 251(59) \times 10^{-11}, \quad (5)$$

which is a 4.2σ deviation of experiment from the SM result. Eq. (5) confirms the Brookhaven result of a discrepancy and further strengthens it, i.e., 4.2σ vs 3.7σ for Brookhaven. Although not yet a discovery of new physics which requires 5σ , Eq. (5) is now more compelling than the Brookhaven result alone as a harbinger of new physics.

In this Letter we investigate if Δa_μ^{FB} given by Eq. (5) can arise from the electroweak sector of supersymmetric models. In the SM the electroweak corrections arise

from the exchange of the W and Z bosons [5, 6]. It is known from early days that supergravity (SUGRA) unified models can generate supersymmetric loop corrections to the muon anomaly from the exchange of charginos and muon-sneutrino, and from the exchange of neutralinos and smuons which can be comparable to the SM electroweak corrections [7, 8]. However, the supersymmetric contribution depends sensitively on the SUGRA parameter space, specifically on the soft parameters [9–12] and an exploration of the parameter space is needed to satisfy the experimental constraint. Thus the Brookhaven experiment [2] led to a number of works [13–17] exploring the parameter space of supersymmetry (SUSY) and supergravity models. Since then the discovery of the Higgs boson at 125 GeV [18, 19] has put further constraint on the parameter space of SUSY models. This is so since at the tree level, supersymmetric models imply that the Higgs boson mass lies below M_Z , and thus one needs a large loop correction to lift the Higgs mass to the experimentally observed value. This in turn implies that the size of weak scale SUSY must be large lying in the several TeV region [20, 21] which further restricts the supergravity models.

In view of the experimental data from Fermilab [1], we investigate in this work the implications of the combined Fermilab and Brookhaven result Δa_μ^{FB} for supergravity models and for discovering supersymmetry at HL-LHC and HE-LHC. To this end, we carry out a comprehensive analysis of the parameter space of supergravity grand unified models [22] using an artificial neural network (ANN). Machine learning methods are found efficient when exploring large parameter spaces (see, e.g., Refs. [23, 24]). Thus our aim is to explore regions of the parameter space of supergravity grand unified models that produce a supersymmetric loop correc-

TABLE I: Input parameters for the benchmarks used in this analysis. All masses are in GeV.

Model	m_0	A_0	m_1	m_2	m_3	$\tan\beta$
(a)	460	-1209	726	378	5590	7.0
(b)	685	1380	868	493	8716	13.0
(c)	682	3033	875	714	8929	123.0
(d)	389	122	649	377	4553	8.2
(e)	254	1039	793	1477	8508	10.8

tion $\Delta a_\mu^{\text{SUSY}}$ consistent with Δa_μ^{FB} . It is found that such regions are those where gluino-driven radiative breaking of the electroweak symmetry occurs [25–27] referred to as \tilde{g} SUGRA. In this region, the sleptons and the electroweakinos can be light while squarks and the extra Higgs bosons of the MSSM, i.e., A^0, H^0, H^\pm are all heavy. The lightest charged particles are the stau, the smuon, the selectron and the chargino. Using a deep neural network (DNN), we investigate the prospects of the discovery of sleptons (smuons and selectrons) at HL-LHC and HE-LHC in the framework of SUGRA grand unified models assuming non-universality of gaugino masses [28–31]. Thus the parameter space of the model consists of $m_0, m_1, m_2, m_3, A_0, \tan\beta$ and $\text{sign}(\mu)$, where m_0 is the universal scalar mass, m_i ($i=1-3$) are the non-universal gaugino masses which are the $U(1)$, $SU(2)$ and $SU(3)$ gaugino masses, A_0 is the universal scalar coupling and $\tan\beta = v_2/v_1$, where v_2 gives mass to the up quarks and v_1 gives mass to the down quarks and the leptons. In the analysis we include the effect of two loop corrections to the a_μ^{SUSY} [32] although such corrections are typically small.

Using ANN we explore the parameter space described above, where $\Delta a_\mu^{\text{SUSY}}$ (arising from chargino and neutralino exchanges) is of size Δa_μ^{FB} . It is found that the desired region of the SUGRA parameter space is one where radiative breaking of the electroweak symmetry is driven by the gluino mass as noted earlier. In Fig. 1 we display Δa_μ arising from supersymmetric loops vs the smuon mass (top panel) and vs the neutralino mass (bottom panel). The Δa_μ constraint with a one sigma corridor arising from the Brookhaven experiment and from the combined Fermilab and Brookhaven data are indicated and it is seen that the SUGRA model points populate the region allowed by the combined data constraint. In the analysis here we have not taken into account SUSY CP phases but we note in passing that SUSY CP phases can have significant effect on the supersymmetric loops corrections [33]. The constraints on SUSY phases arising from Δa_μ^{FB} are discussed in the Supplemental Material.

Sparticle spectrum constrained by Δa_μ^{FB} : As noted already the slepton and weakino mass spectrum arising from the Δa_μ^{FB} constraint lie in the region of the parameter space with light and heavy particles, where the light particles with masses in the few hundred GeV range

TABLE II: The light sparticle spectrum consisting of smuon ($\tilde{\mu}$), muon sneutrino ($\tilde{\nu}_\mu$), neutralino ($\tilde{\chi}_1^0$), chargino ($\tilde{\chi}_1^\pm$) contributing to the muon $g-2$, the DM relic density, Δa_μ (calculated at the two-loop level using **GM2Ca1c** [34]) and the branching ratio (BR) of $\tilde{\ell} \rightarrow \ell \tilde{\chi}_1^0$.

Model	$\tilde{\mu}$	$\tilde{\nu}_\mu$	$\tilde{\chi}_1^0$	$\tilde{\chi}_1^\pm$	$\Delta a_\mu \times 10^{-9}$	Ωh^2	BR
(a)	313	304	222.2	222.4	2.13	0.001	33%
(b)	412	405	271.7	271.9	3.04	0.002	32%
(c)	501	495	331.0	465.0	2.02	0.055	65%
(d)	305	295	237.4	237.6	2.33	0.002	31%
(e)	721	716	300	1143	2.56	0.052	100%

consisting of the neutralino, the chargino, the smuon and smuon-neutrino produce a significant correction to $\Delta a_\mu^{\text{SUSY}}$ while the sparticles with color, and the remaining spectrum are significantly heavy lying in the several TeV region and do not participate in the loop corrections. The mass range of the light particles is shown in Fig. 2 where the top panel exhibits an illustrative mass range for the case when the chargino is the NLSP while the bottom panel is the case when the stau is the NLSP. The analysis shows that an smuon mass up to ~ 1 TeV, a chargino up to ~ 1.5 TeV and a neutralino up to ~ 400 GeV are allowed while being consistent with all constraints including Δa_μ^{FB} and the current LHC limits.

Dark matter: Δa_μ^{FB} also puts significant constraints on the spin-independent neutralino-nucleon cross section σ_{SI} . As shown in the top panel of Fig. 3 one finds that some of the models have σ_{SI} within reach of DARWIN [35] and are thus discoverable. However, most of the allowed parameter space consistent with the Δa_μ^{FB} constraint lies below the neutrino floor. The smallness of the σ_{SI} is a direct consequence of the fact that the neutralino is mostly a bino with only a small wino content.

Implications of Δa_μ^{FB} for discovering SUSY at HL-LHC and HE-LHC: The light sleptons appearing in Table II could be pair produced in proton-proton collisions at 14 TeV (HL-LHC) and 27 TeV (HE-LHC). The production cross-sections are computed at aNNLO+NNLL accuracy using **Resummino-3.0** [36, 37] and the five-flavor NNPDF23NLO PDF set and given in Table III. The signal and background events are simulated with **MadGraph5_aMC@NLO-3.1.0** [38] and showered with **PYTHIA8** [39]. Detector simulation and event reconstruction is handled by **Delphes-3.4.2** [40]. The signal region consists of identifying two light leptons of same flavor and opposite sign (SFOS), missing transverse energy (MET) and at least two jets ($N \geq 2$) in the final state. We call the signal region **SR-2ℓNj** with four variations A, B, C and D depending on the center-of-mass energy and the smuon-neutralino mass gap those signal regions target. The selected SFOS leptons, non b-tagged jets and MET must pass a preselection criteria in both signal and background events. We employ a deep neural

TABLE III: The aNNLO+NNLL pair production cross-sections, in fb, of sleptons at $\sqrt{s} = 14$ TeV and at $\sqrt{s} = 27$ TeV for benchmarks (a)–(e) of Table I.

Model	$\sigma(pp \rightarrow \tilde{e}_L \tilde{e}_L)$		$\sigma(pp \rightarrow \tilde{\mu}_L \tilde{\mu}_L)$	
	14 TeV	27 TeV	14 TeV	27 TeV
(a)	4.41	14.0	4.42	14.0
(b)	1.39	5.07	1.40	5.09
(c)	0.58	2.38	0.58	2.39
(d)	4.90	15.4	4.91	15.4
(e)	0.095	0.54	0.096	0.54

network implemented in ROOT's [41] own TMVA [42] to train the signal (S) and background (B) events using a set of kinematic variables. The result is a new variable called 'DNN response' which can be used to reject events thus maximizing the $S/\sqrt{S+B}$ ratio. Fig. 4 shows a distribution in the DNN response for benchmark (a) at 14 TeV and 27 TeV. The DNN has successfully separated the signal events which can be seen peaking near 1 and above the SM background. A cut on DNN response > 0.9 removes most of the background and point (a) becomes discoverable at HL-LHC with 1460 fb^{-1} of integrated luminosity while requiring $\sim 1000 \text{ fb}^{-1}$ at HE-LHC. Using the same techniques, benchmark (b) can be discovered with $\mathcal{L} \sim 1008 \text{ fb}^{-1}$ at HL-LHC and $\sim 400 \text{ fb}^{-1}$ at HE-LHC. All points except (e) are discoverable at both machines while (e) requires $\sim 4750 \text{ fb}^{-1}$ at HE-LHC (see Fig. 5 which illustrates the different required integrated luminosities).

Conclusion: In this Letter we have shown that the combined Fermilab and Brookhaven data on $a_\mu^{\text{exp}} - a_\mu^{\text{SM}}$ has important implications for the discovery of supersymmetry at HL-LHC and HE-LHC. Specifically, exploration of the SUGRA parameter space using machine learning shows that the combined Fermilab and Brookhaven Δa_μ^{FB} constraint indicates that the favored region of the SUGRA parameter space is one where gluino-driven radiative breaking of the electroweak symmetry occurs. In this region the renormalization group analysis leads to a split light and heavy mass spectrum where the electroweak gauginos and the sleptons are light lying in the few hundred GeV range, while the remaining mass spectrum is heavy. The light spectrum which includes the neutralino, the chargino, the smuon, and the smuon-neutrino can produce a correction to the muon anomaly consistent with Δa_μ^{FB} . Further, the light stau and the chargino are seen to be the lightest charged particles while the sleptons are light enough to be prime candidates for discovery at HL-LHC and HE-LHC. We perform a signal region analysis and compute the integrated luminosity needed for SUSY discovery. It is shown that supergravity models which produce a correction to Δa_μ^{SM} of size indicated Δa_μ^{FB} are discoverable at HL-LHC within the optimal integrated luminosity and with a smaller in-

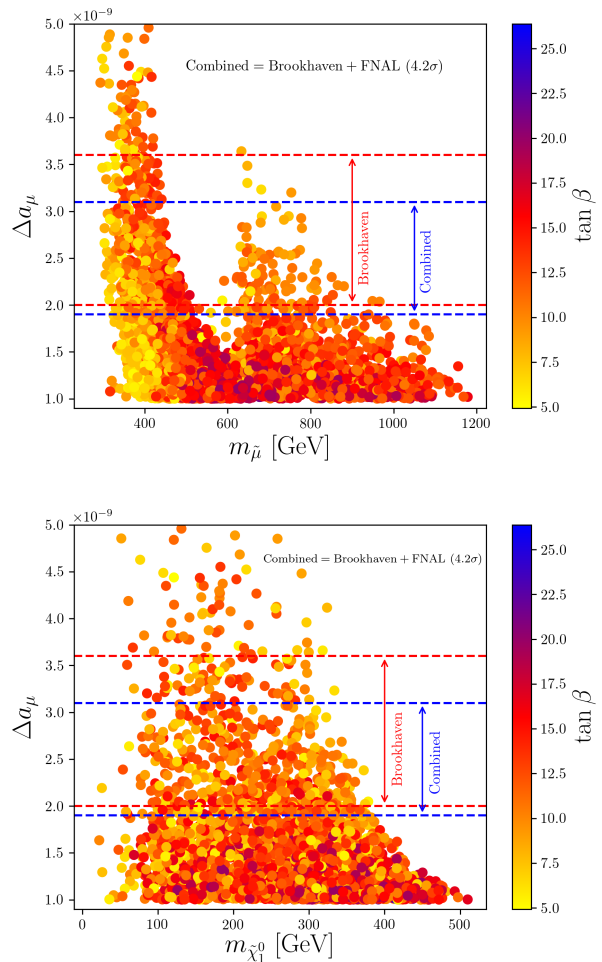


FIG. 1: $\Delta a_\mu^{\text{SUSY}}$ arising from the SUGRA parameter space using an artificial neural network as part of xBIT [43]. The points satisfy the Higgs boson mass, the dark matter relic density and limits from dark matter direct detection experiments and the LHC. One sigma error corridor on Δa_μ experimental result from Brookhaven (red dashed lines) and from the combined Fermilab and Brookhaven result (blue dashed lines) are also displayed.

tegrated luminosity at HE-LHC.

The research of AA and MK was supported by the BMBF under contract 05H18PMCC1. The research of PN was supported in part by the NSF Grant PHY-191332.

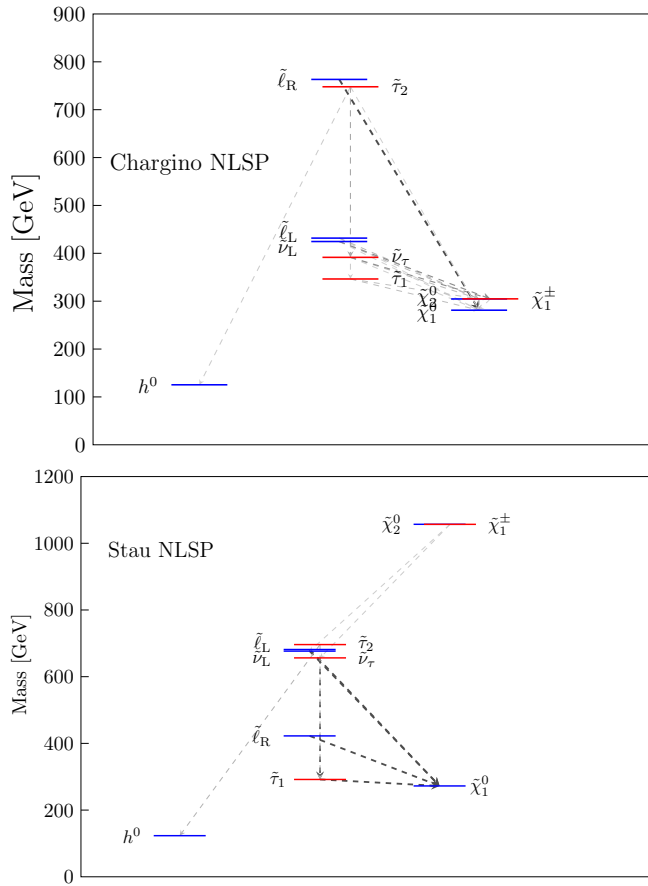


FIG. 2: Exhibition of the light sparticle spectrum in \tilde{g} SUGRA models constrained by Δa_μ^{FB} . The top panel is for the case of chargino NLSP and bottom panel is for the stau NLSP.

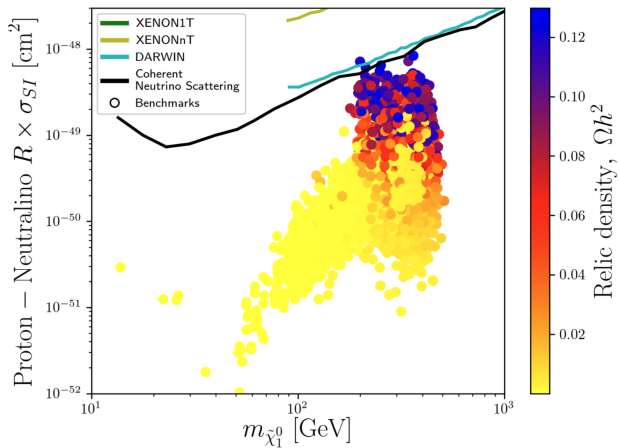


FIG. 3: Upper panel: Spin-independent proton-neutralino cross section σ_{SI} as a function of the neutrino mass constrained by Δa_μ^{FB} . Here $R = \Omega h^2 / (\Omega h^2)_{\text{Planck}}$ where $(\Omega h^2)_{\text{Planck}} \sim 0.12$.

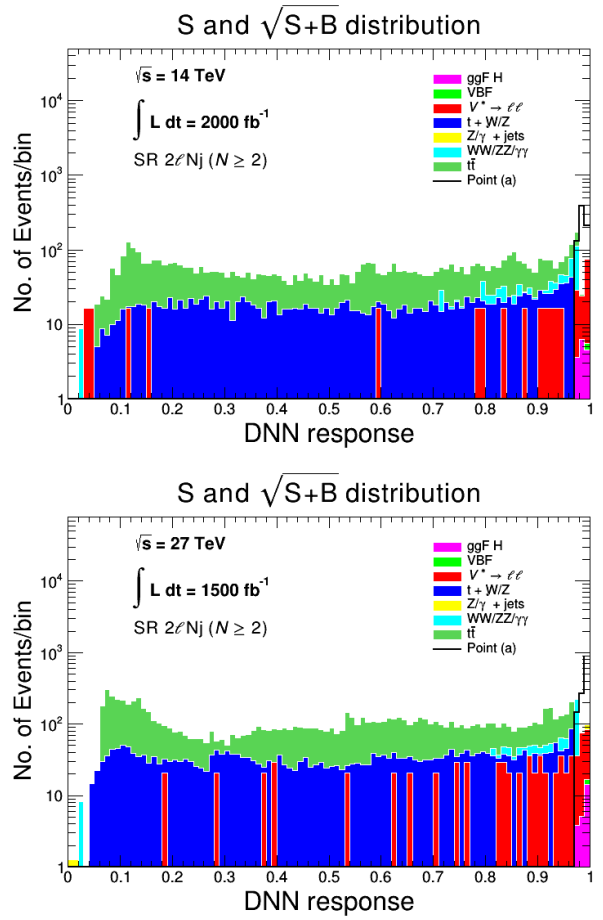


FIG. 4: Distributions in the DNN response for the signal and background events pertaining to benchmark (a) at 14 TeV (top panel) and 27 TeV (bottom panel).

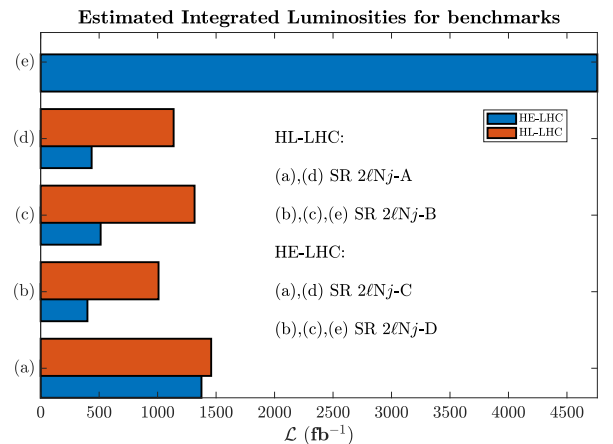


FIG. 5: The integrated luminosities needed for discovery of SUSY at HL-LHC and HE-LHC assuming that Δa_μ^{FB} arises from SUSY loops. The signal regions SR-2 ℓ Nj-A and SR-2 ℓ Nj-C target small smuon-neutralino mass gaps ($\lesssim 90$ GeV) and SR-2 ℓ Nj-B and SR-2 ℓ Nj-D target larger mass gaps.

-
- * Email: aabouibr@uni-muenster.de; ORCID: 0000-0002-1110-4265
- † Email: michael.klasen@uni-muenster.de; ORCID: 0000-0002-4665-3088
- ‡ Email: p.nath@northeastern.edu; ORCID: 0000-0001-9879-9751
- [1] B. Abi, T. Albahri, S. Al-Kilani, D. Allspach, L. P. Alonzi, A. Anastasi, A. Anisenkov, F. Azfar, K. Badgley and S. Baessler, *et al.* doi:10.1103/PhysRevLett.126.141801 [arXiv:2104.03281 [hep-ex]].
- [2] G. W. Bennett *et al.* [Muon g-2], Phys. Rev. D **73**, 072003 (2006) doi:10.1103/PhysRevD.73.072003 [arXiv:hep-ex/0602035 [hep-ex]].
- [3] M. Tanabashi, *et al.*, Review of Particle Physics, Phys. Rev. D **98** (3) (2018) 030001. doi:10.1103/PhysRevD.98.030001
- [4] T. Aoyama, N. Asmussen, M. Benayoun, J. Bijnens, T. Blum, M. Bruno, I. Caprini, C. M. Carloni Calame, M. Cè and G. Colangelo, *et al.* Phys. Rept. **887**, 1-166 (2020) doi:10.1016/j.physrep.2020.07.006 [arXiv:2006.04822 [hep-ph]].
- [5] K. Fujikawa, B. W. Lee, and A. I. Sanda, Phys. Rev. **D6**, 2923 (1972); R. Jackiw and S. Weinberg, Phys. Rev. **D5**, 2473 (1972); G. Altarelli, N. Cabibbo, and L. Maiani, Phys. Lett. **B40**, 415 (1972); I. Bars and M. Yoshimura, Phys. Rev. **D6**, 374 (1972); W. A. Bardeen, R. Gastmans, and B. E. Lautrup, Nucl. Phys. **B46**, 315 (1972).
- [6] A. Czarnecki, B. Krause and W. J. Marciano, Phys. Rev. Lett. **76**, 3267-3270 (1996) doi:10.1103/PhysRevLett.76.3267 [arXiv:hep-ph/9512369 [hep-ph]].
- [7] D. A. Kosower, L. M. Krauss and N. Sakai, Phys. Lett. B **133**, 305-310 (1983) doi:10.1016/0370-2693(83)90152-1
- [8] T. C. Yuan, R. L. Arnowitt, A. H. Chamseddine and P. Nath, Z. Phys. C **26**, 407 (1984) doi:10.1007/BF01452567
- [9] J. L. Lopez, D. V. Nanopoulos and X. Wang, Phys. Rev. D **49**, 366-372 (1994) doi:10.1103/PhysRevD.49.366 [arXiv:hep-ph/9308336 [hep-ph]].
- [10] U. Chattopadhyay and P. Nath, Phys. Rev. D **53**, 1648-1657 (1996) doi:10.1103/PhysRevD.53.1648 [arXiv:hep-ph/9507386 [hep-ph]].
- [11] T. Moroi, Phys. Rev. D **53**, 6565-6575 (1996) [erratum: Phys. Rev. D **56**, 4424 (1997)] doi:10.1103/PhysRevD.53.6565 [arXiv:hep-ph/9512396 [hep-ph]].
- [12] M. Carena, G. F. Giudice and C. E. M. Wagner, Phys. Lett. B **390**, 234-242 (1997) doi:10.1016/S0370-2693(96)01396-2 [arXiv:hep-ph/9610233 [hep-ph]].
- [13] A. Czarnecki and W. J. Marciano, Phys. Rev. D **64**, 013014 (2001) doi:10.1103/PhysRevD.64.013014 [arXiv:hep-ph/0102122 [hep-ph]].
- [14] U. Chattopadhyay and P. Nath, Phys. Rev. Lett. **86**, 5854-5857 (2001) doi:10.1103/PhysRevLett.86.5854 [arXiv:hep-ph/0102157 [hep-ph]].
- [15] L. L. Everett, G. L. Kane, S. Rigolin and L. T. Wang, Phys. Rev. Lett. **86**, 3484-3487 (2001) doi:10.1103/PhysRevLett.86.3484 [arXiv:hep-ph/0102145 [hep-ph]].
- [16] J. L. Feng and K. T. Matchev, Phys. Rev. Lett. **86**, 3480-3483 (2001) doi:10.1103/PhysRevLett.86.3480 [arXiv:hep-ph/0102146 [hep-ph]].
- [17] E. A. Baltz and P. Gondolo, Phys. Rev. Lett. **86**, 5004 (2001) doi:10.1103/PhysRevLett.86.5004 [arXiv:hep-ph/0102147 [hep-ph]].
- [18] S. Chatrchyan *et al.* [CMS], Phys. Lett. B **716**, 30-61 (2012) doi:10.1016/j.physletb.2012.08.021 [arXiv:1207.7235 [hep-ex]].
- [19] G. Aad *et al.* [ATLAS], Phys. Lett. B **716**, 1-29 (2012) doi:10.1016/j.physletb.2012.08.020 [arXiv:1207.7214 [hep-ex]].
- [20] S. Akula, B. Altunkaynak, D. Feldman, P. Nath and G. Peim, Phys. Rev. D **85**, 075001 (2012) doi:10.1103/PhysRevD.85.075001 [arXiv:1112.3645 [hep-ph]].
- [21] A. Arbey, M. Battaglia, A. Djouadi, F. Mahmoudi and J. Quevillon, Phys. Lett. B **708**, 162 (2012); H. Baer, V. Barger and A. Mustafayev, Phys. Rev. D **85**, 075010 (2012); J. Ellis and K. A. Olive, Eur. Phys. J. C **72**, 2005 (2012); S. Heinemeyer, O. Stal and G. Weiglein, Phys. Lett. B **710**, 201 (2012);
- [22] A. H. Chamseddine, R. Arnowitt and P. Nath, Phys. Rev. Lett. **49** (1982) 970; P. Nath, R. L. Arnowitt and A. H. Chamseddine, Nucl. Phys. B **227**, 121 (1983); L. J. Hall, J. D. Lykken and S. Weinberg, Phys. Rev. D **27**, 2359 (1983). doi:10.1103/PhysRevD.27.2359
- [23] J. Hollingsworth, M. Ratz, P. Tanedo and D. Whiteson, [arXiv:2103.06957 [hep-th]].
- [24] C. Balázs *et al.* [DarkMachines High Dimensional Sampling Group], [arXiv:2101.04525 [hep-ph]].
- [25] S. Akula and P. Nath, Phys. Rev. D **87**, no.11, 115022 (2013) doi:10.1103/PhysRevD.87.115022 [arXiv:1304.5526 [hep-ph]].
- [26] A. Aboubrahim and P. Nath, Phys. Rev. D **100**, no.1, 015042 (2019) doi:10.1103/PhysRevD.100.015042 [arXiv:1905.04601 [hep-ph]].
- [27] A. Aboubrahim, P. Nath and R. M. Syed, JHEP **01**, 047 (2021) doi:10.1007/JHEP01(2021)047 [arXiv:2005.00867 [hep-ph]].
- [28] J. R. Ellis, K. Enqvist, D. V. Nanopoulos and K. Tamvakis, Phys. Lett. B **155**, 381-386 (1985) doi:10.1016/0370-2693(85)91591-6
- [29] A. Corsetti and P. Nath, Phys. Rev. D **64**, 125010 (2001); A. Birkedal-Hansen and B. D. Nelson, Phys. Rev. D **67**, 095006 (2003); G. Belanger, F. Boudjema, A. Cottrant, A. Pukhov and A. Semenov, Nucl. Phys. B **706**, 411 (2005); H. Baer, A. Mustafayev, E. K. Park, S. Profumo and X. Tata, JHEP **04** (2006), 041 doi:10.1088/1126-6708/2006/04/041 [arXiv:hep-ph/0603197 [hep-ph]]; I. Gogoladze, F. Nasir, Q. Shafi and C. S. Un, Phys. Rev. D **90**, no. 3, 035008 (2014) doi:10.1103/PhysRevD.90.035008; S. P. Martin, Phys. Rev. D **79**, 095019 (2009) doi:10.1103/PhysRevD.79.095019
- [30] D. Feldman, Z. Liu and P. Nath, Phys. Rev. D **80**, 015007 (2009) doi:10.1103/PhysRevD.80.015007 [arXiv:0905.1148 [hep-ph]].
- [31] A. S. Belyaev, S. F. King and P. B. Schaefer, Phys. Rev. D **97**, no.11, 115002 (2018) doi:10.1103/PhysRevD.97.115002 [arXiv:1801.00514 [hep-ph]].
- [32] S. Heinemeyer, D. Stockinger and G. Weiglein, Nucl. Phys. B **690**, 62-80 (2004) doi:10.1016/j.nuclphysb.2004.04.017 [arXiv:hep-

- ph/0312264 [hep-ph]].
- [33] A. Aboubrahim, T. Ibrahim and P. Nath, *Phys. Rev. D* **94**, no.1, 015032 (2016) doi:10.1103/PhysRevD.94.015032 [arXiv:1606.08336 [hep-ph]].
- [34] P. Athron, M. Bach, H. G. Fargnoli, C. Gnendiger, R. Greifenhagen, J. h. Park, S. Paßehr, D. Stöckinger, H. Stöckinger-Kim and A. Voigt, *Eur. Phys. J. C* **76**, no.2, 62 (2016) doi:10.1140/epjc/s10052-015-3870-2 [arXiv:1510.08071 [hep-ph]].
- [35] C. Macolino [DARWIN], *J. Phys. Conf. Ser.* **1468**, no.1, 012068 (2020) doi:10.1088/1742-6596/1468/1/012068
- [36] J. Debove, B. Fuks and M. Klasen, *Nucl. Phys. B* **849**, 64-79 (2011) doi:10.1016/j.nuclphysb.2011.03.015 [arXiv:1102.4422 [hep-ph]].
- [37] B. Fuks, M. Klasen, D. R. Lamprea and M. Rothering, *Eur. Phys. J. C* **73**, 2480 (2013) doi:10.1140/epjc/s10052-013-2480-0 [arXiv:1304.0790 [hep-ph]].
- [38] J. Alwall, R. Frederix, S. Frixione, V. Hirschi, F. Maltoni, O. Mattelaer, H. S. Shao, T. Stelzer, P. Torrielli and M. Zaro, *JHEP* **07**, 079 (2014) doi:10.1007/JHEP07(2014)079 [arXiv:1405.0301 [hep-ph]].
- [39] T. Sjöstrand, S. Ask, J. R. Christiansen, R. Corke, N. Desai, P. Ilten, S. Mrenna, S. Prestel, C. O. Rasmussen and P. Z. Skands, *Comput. Phys. Commun.* **191**, 159-177 (2015) doi:10.1016/j.cpc.2015.01.024 [arXiv:1410.3012 [hep-ph]].
- [40] J. de Favereau *et al.* [DELPHES 3], *JHEP* **02**, 057 (2014) doi:10.1007/JHEP02(2014)057 [arXiv:1307.6346 [hep-ex]].
- [41] I. Antcheva, M. Ballintijn, B. Bellenot, M. Biskup, R. Brun, N. Buncic, P. Canal, D. Casadei, O. Couet and V. Fine, *et al. Comput. Phys. Commun.* **182**, 1384-1385 (2011) doi:10.1016/j.cpc.2011.02.008
- [42] P. Speckmayer, A. Hocker, J. Stelzer and H. Voss, *J. Phys. Conf. Ser.* **219**, 032057 (2010) doi:10.1088/1742-6596/219/3/032057
- [43] F. Staub, [arXiv:1906.03277 [hep-ph]].
- [44] W. Porod, *Comput. Phys. Commun.* **153**, 275-315 (2003) doi:10.1016/S0010-4655(03)00222-4 [arXiv:hep-ph/0301101 [hep-ph]].
- [45] W. Porod and F. Staub, *Comput. Phys. Commun.* **183**, 2458-2469 (2012) doi:10.1016/j.cpc.2012.05.021 [arXiv:1104.1573 [hep-ph]].
- [46] G. Bélanger, F. Boudjema, A. Pukhov and A. Semenov, *Comput. Phys. Commun.* **192**, 322-329 (2015) doi:10.1016/j.cpc.2015.03.003 [arXiv:1407.6129 [hep-ph]].
- [47] J. Bernon and B. Dumont, *Eur. Phys. J. C* **75**, no.9, 440 (2015) doi:10.1140/epjc/s10052-015-3645-9 [arXiv:1502.04138 [hep-ph]].
- [48] S. Kraml, T. Q. Loc, D. T. Nhung and L. Ninh, *SciPost Phys.* **7**, no.4, 052 (2019) doi:10.21468/SciPostPhys.7.4.052 [arXiv:1908.03952 [hep-ph]].
- [49] P. Bechtle, S. Heinemeyer, O. Stal, T. Stefaniak and G. Weiglein, *Eur. Phys. J. C* **74**, no.2, 2711 (2014) doi:10.1140/epjc/s10052-013-2711-4 [arXiv:1305.1933 [hep-ph]].
- [50] P. Bechtle, D. Dercks, S. Heinemeyer, T. Klingl, T. Stefaniak, G. Weiglein and J. Wittbrodt, *Eur. Phys. J. C* **80**, no.12, 1211 (2020) doi:10.1140/epjc/s10052-020-08557-9 [arXiv:2006.06007 [hep-ph]].
- [51] C. K. Khosa, S. Kraml, A. Lessa, P. Neuhuber and W. Waltenberger, doi:10.31526/lhep.2020.158 [arXiv:2005.00555 [hep-ph]].
- [52] S. Kraml, S. Kulkarni, U. Laa, A. Lessa, W. Magerl, D. Proschofsky-Spindler and W. Waltenberger, *Eur. Phys. J. C* **74**, 2868 (2014) doi:10.1140/epjc/s10052-014-2868-5 [arXiv:1312.4175 [hep-ph]].
- [53] S. Kraml, S. Kulkarni, U. Laa, A. Lessa, V. Magerl, W. Magerl, D. Proschofsky-Spindler, M. Traub and W. Waltenberger, [arXiv:1412.1745 [hep-ph]].
- [54] D. Barducci, G. Belanger, J. Bernon, F. Boudjema, J. Da Silva, S. Kraml, U. Laa and A. Pukhov, *Comput. Phys. Commun.* **222**, 327-338 (2018) doi:10.1016/j.cpc.2017.08.028 [arXiv:1606.03834 [hep-ph]].
- [55] A. Buckley, J. Ferrando, S. Lloyd, K. Nordström, B. Page, M. Rüfenacht, M. Schönherr and G. Watt, *Eur. Phys. J. C* **75**, 132 (2015) doi:10.1140/epjc/s10052-015-3318-8 [arXiv:1412.7420 [hep-ph]].
- [56] M. Cacciari, G. P. Salam and G. Soyez, *Eur. Phys. J. C* **72**, 1896 (2012) doi:10.1140/epjc/s10052-012-1896-2 [arXiv:1111.6097 [hep-ph]].
- [57] M. Cacciari, G. P. Salam and G. Soyez, *JHEP* **04**, 063 (2008) doi:10.1088/1126-6708/2008/04/063 [arXiv:0802.1189 [hep-ph]].
- [58] C. G. Lester and D. J. Summers, *Phys. Lett. B* **463**, 99-103 (1999) doi:10.1016/S0370-2693(99)00945-4 [arXiv:hep-ph/9906349 [hep-ph]].
- [59] A. Barr, C. Lester and P. Stephens, *J. Phys. G* **29**, 2343-2363 (2003) doi:10.1088/0954-3899/29/10/304 [arXiv:hep-ph/0304226 [hep-ph]].
- [60] C. G. Lester and B. Nachman, *JHEP* **03**, 100 (2015) doi:10.1007/JHEP03(2015)100 [arXiv:1411.4312 [hep-ph]].
- [61] T. Ibrahim and P. Nath, *Phys. Rev. D* **62**, 015004 (2000) doi:10.1103/PhysRevD.62.015004 [arXiv:hep-ph/9908443 [hep-ph]].
- [62] T. Ibrahim, U. Chattopadhyay and P. Nath, *Phys. Rev. D* **64**, 016010 (2001) doi:10.1103/PhysRevD.64.016010 [arXiv:hep-ph/0102324 [hep-ph]].

What Fermilab $(g - 2)_\mu$ experiment tells us about discovering SUSY at HL(E)-LHC

Supplemental Material

Amin Aboubrahim, Michael Klasen and Pran Nath

SCAN AND CONSTRAINTS ON THE SUGRA PARAMETER SPACE

The scan of the SUGRA parameter space can be optimized by using a machine learning algorithm with constraints on the Higgs mass, the dark matter relic density and the muon $g - 2$. We use an artificial neural network (ANN) implemented in `xBit` [43] interfaced with `SPheno-4.0.4` [44, 45] which uses two-loop MSSM RGEs and three-loop standard model RGEs and takes into account SUSY threshold effects at the one-loop level to generate the sparticle spectrum and `micrOMEGAs-5.2.7` [46] to calculate the DM relic density and the spin-independent scattering cross section. The ANN used has three layers with 25 neurons per layer. With the above constraints imposed while allowing for a 2σ window, the ANN constructs the likelihood function of a point from the three constraints and the training is done on the likelihood rather than on the observable itself. The obtained set of points are then passed to `Lilith` [47, 48], `HiggsSignals` [49] and `HiggsBounds` [50] to check the Higgs sector constraints as well as `SModelS` [51–53] to check the LHC constraints. Furthermore, `micrOMEGAs-5.2.7` [54] has a module which we use to check the constraints from DM direct detection experiments. The points passing all those constraints are plotted in Figs. 1 and S1.

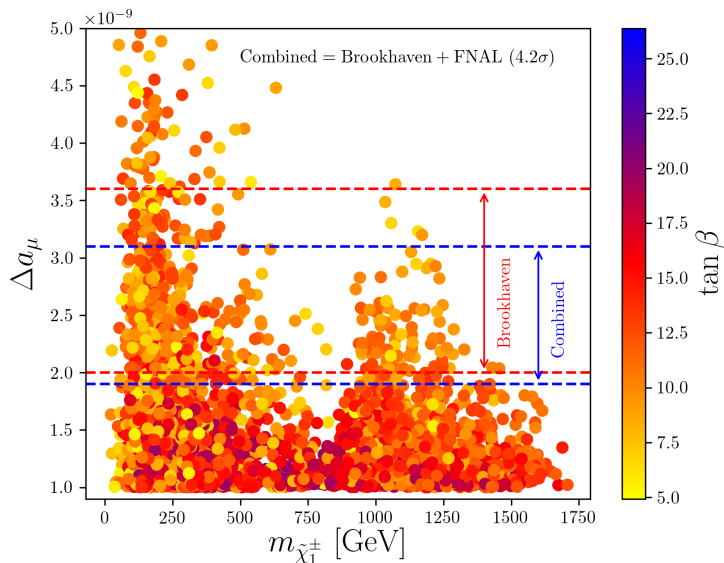


FIG. S1: A scatter plot of Δa_μ versus the chargino mass as a result of a scan of the SUGRA parameter space using an artificial neural network. The points satisfy the Higgs boson mass, the dark matter relic density and limits from dark matter direct detection experiments and the LHC.

LHC ANALYSIS

Slepton (selectron and smuon) pair production is a notoriously difficult signal region to look for at the LHC owing to their small production cross section and the decay topology resembling the SM backgrounds. The muon $g - 2$ prefers smuons with mass less than 1 TeV as one can see from Fig. 1 and their direct detection at the LHC is of importance especially after the recent $(g - 2)_\mu$ results from Fermilab. Our signal consists of smuon and selectron pair production which decay to light leptons (electrons and muons) and a neutralino. The final states which make up our signal region

involve two same flavor and opposite sign (SFOS) leptons with missing transverse energy (MET). We also require at least two jets which can be used to trigger on especially in an ISR-assisted topology when the MET is small. For such final states, the dominant SM backgrounds are from diboson production, Z/γ +jets, dilepton production from off-shell vector bosons ($V^* \rightarrow \ell\ell$), $t\bar{t}$ and $t + W/Z$. The subdominant backgrounds are Higgs production via gluon fusion (ggF H) and vector boson fusion (VBF). The simulation of the signal and background events is performed at LO with `MadGraph5_aMC@NLO-3.1.0` interfaced to `LHAPDF` [55] using the `NNPDF30LO` PDF set. Up to two hard jets are added at generator level. The parton level events are passed to `PYTHIA8` [39] for showering and hadronization using a five-flavor matching scheme in order to avoid double counting of jets. For the signal events, the matching/merging scale is set at one-fourth the mass of the pair produced sleptons. Additional jets from ISR and FSR are added to the signal and background events. Jets are clustered with `FastJet` [56] using the anti- k_t algorithm [57] with jet radius $R = 0.4$. `DELPHES-3.4.2` [40] is then employed for detector simulation and event reconstruction using the HL-LHC and HE-LHC card. The SM backgrounds are scaled to their relevant NLO cross sections while aNNLO+NNLL cross sections are used for the signal events. The latter are calculated with `Resummino-3.0` [36, 37] using the five-flavor `NNPDF23NLO` PDF set.

The discrimination between the signal and background events is done with the help of a deep neural network (DNN) as part of the ‘Toolkit for Multivariate Analysis’ (TMVA) [42] framework within `ROOT6` [41]. To train the signal and background events, we use a set of discriminating variables:

1. E_T^{miss} : the missing transverse energy in the event. It is usually high for the signal due to the presence of neutralinos.
2. The transverse momentum of the leading non-b tagged jets, $p_T(j_1)$. Rejecting b-tagged jets reduces the $t\bar{t}$ background.
3. The transverse momentum of the leading lepton (electron or muon), $p_T(\ell_1)$.
4. The transverse momentum of the ISR jet, p_T^{ISR} .
5. M_{T2} , the stransverse mass [58–60] of the leading and subleading leptons

$$M_{T2} = \min \left[\max \left(m_T(\mathbf{p}_T^{\ell_1}, \mathbf{q}_T), m_T(\mathbf{p}_T^{\ell_2}, \mathbf{p}_T^{\text{miss}} - \mathbf{q}_T) \right) \right], \quad (\text{S1})$$

where \mathbf{q}_T is an arbitrary vector chosen to find the appropriate minimum and the transverse mass m_T is given by

$$m_T(\mathbf{p}_{T1}, \mathbf{p}_{T2}) = \sqrt{2(p_{T1} p_{T2} - \mathbf{p}_{T1} \cdot \mathbf{p}_{T2})}. \quad (\text{S2})$$

6. The quantity M_T^{min} defined as $M_T^{\text{min}} = \min[m_T(\mathbf{p}_T^{\ell_1}, \mathbf{p}_T^{\text{miss}}), m_T(\mathbf{p}_T^{\ell_2}, \mathbf{p}_T^{\text{miss}})]$. The variables M_{T2} and M_T^{min} are effective when dealing with large MET in the final state.
7. The dilepton invariant mass, $m_{\ell\ell}$, helps in rejecting the diboson background with a peak near the Z boson mass which can be done by setting $m_{\ell\ell} > 100$ GeV.
8. The opening angle between the MET system and the dilepton system, $\Delta\phi(\mathbf{p}_T^\ell, \mathbf{p}_T^{\text{miss}})$, where $\mathbf{p}_T^\ell = \mathbf{p}_T^{\ell_1} + \mathbf{p}_T^{\ell_2}$.
9. The smallest opening angle between the first three leading jets in an event and the MET system, $\Delta\phi_{\text{min}}(\mathbf{p}_T(j_i), \mathbf{p}_T^{\text{miss}})$, where $i = 1, 2, 3$.

Fig. S2 shows normalized distributions in six of the discriminating variables which are used by the DNN for training. Before the events are fed into a DNN, a set of preselection criteria is applied to the signal and background. The leading and subleading leptons must have a transverse momenta $p_T > 15$ GeV for electrons and $p_T > 10$ GeV for muons with $|\eta| < 2.5$. Each event should contain at least two non-b-tagged jets with the leading $p_T > 20$ GeV in the $|\eta| < 2.4$ region and $E_T^{\text{miss}} > 100$ GeV. Two statistically independent sets of signal and background events are used for training and testing of a four-layer DNN. The training phase uses the above set of variables to create a new powerful kinematic variable called the ‘DNN response’ which can be used as a discriminant, effectively rejecting most of the SM background. Distributions in the ‘DNN response’ variable are shown in Figs. 4 and S3. The cut on the DNN response is aided by a series of analysis cuts using some of the variables described above. A summary of the preselection criteria and the analysis cuts is given in Table S1. Notice that the cuts need to be customized when studying HE-LHC as compared to HL-LHC. Furthermore, we consider two signal regions (SR) for each center-of-mass

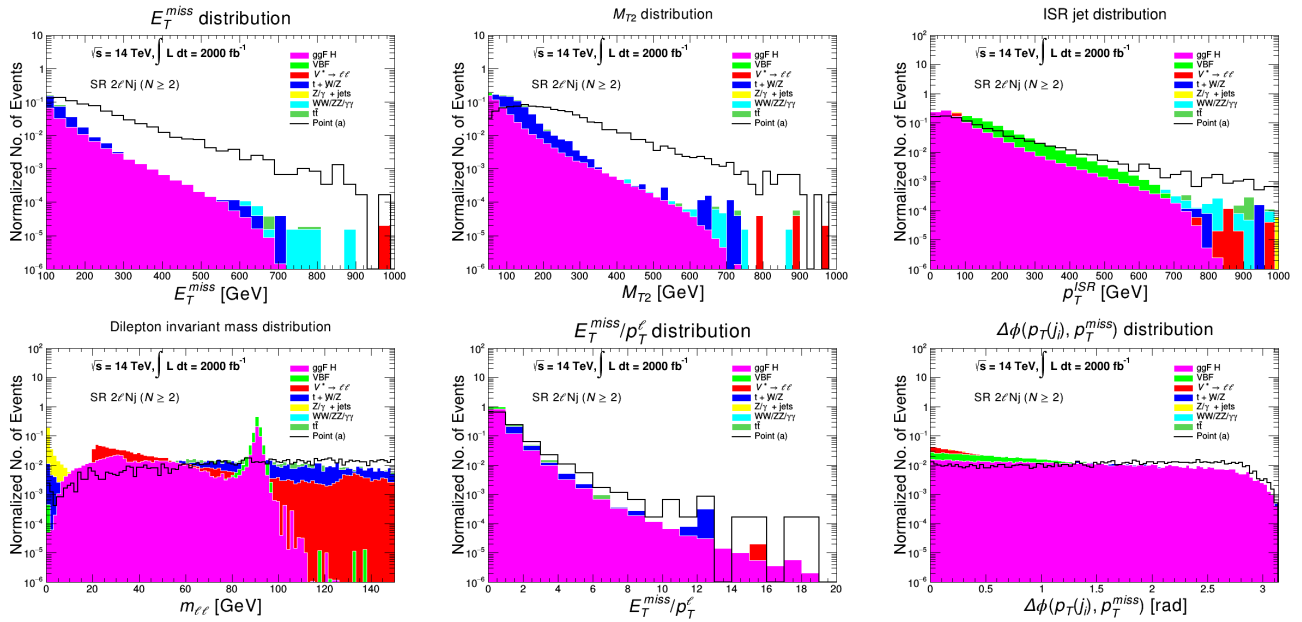


FIG. S2: A sample of the discriminating variables using by the DNN for training and testing. The distributions are in the normalized number of events scaled by a specific integrated luminosity to show the discriminating power of each variable.

energy. The signal regions SR-2 ℓ Nj-A and SR-2 ℓ Nj-C target small smuon-neutralino mass gaps ($\lesssim 90$ GeV) and SR-2 ℓ Nj-B and SR-2 ℓ Nj-D target larger mass gaps.

Observable	SR-2 ℓ Nj-A	SR-2 ℓ Nj-B	SR-2 ℓ Nj-C	SR-2 ℓ Nj-D
	14 TeV		27 TeV	
Preselection criteria				
N_ℓ (SFOS)	2		2	
$N_{\text{non-b-tagged}}$	≥ 2		≥ 2	
$p_T^{\text{leading jet}}$ [GeV]	> 20		> 20	
p_T^ℓ (electron, muon) [GeV]	$> 15, > 10$		$> 15, > 10$	
E_T^{miss} [GeV]	> 100		> 100	
Analysis cuts				
p_T^{ISR} [GeV]	> 100	> 100	> 120	> 120
$\Delta\phi_{\text{min}}(\mathbf{p}_T(j_i), \mathbf{p}_T^{\text{miss}})$ [rad]	> 1.5	> 1.5	> 1.8	> 1.8
M_{T2} [GeV]	> 100	> 120	> 110	> 150
$m_{\ell\ell}$ [GeV]	> 105	> 105	> 115	> 115
DNN response	> 0.95	> 0.92	> 0.92	> 0.9

TABLE S1: Preselection and analysis cuts (at 14 TeV and 27 TeV) applied to the signal and SM backgrounds for two signal regions targeting optimized depending on the smuon-neutralino mass gap.

CONSTRAINTS ON CP PHASES FROM Δa_μ^{FB}

It is known that SUSY CP violating phases arising from the soft parameters can have significant effect on a_μ^{SUSY} [61, 62]. Here we discuss the phase dependence of the chargino contribution which is the dominant one, although the analysis is done including both the chargino and the neutralino exchange contributions. For the chargino exchange

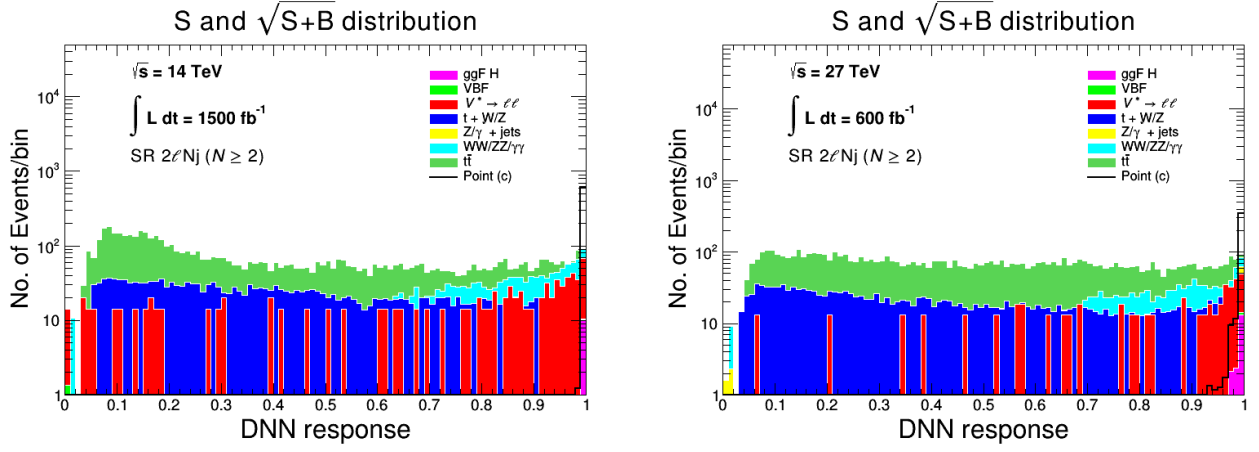


FIG. S3: Distributions in the DNN response for the signal and background events pertaining to benchmark (c) at 14 TeV (left panel) and 27 TeV (right panel).

contribution the phases enter via the chargino mass matrix

$$M_C = \begin{pmatrix} |m_2|e^{i\xi_2} & \sqrt{2}m_W \sin\beta \\ \sqrt{2}m_W \cos\beta & |\mu|e^{i\theta_\mu} \end{pmatrix}, \quad (\text{S3})$$

where θ_μ is the phase of the Higgs mixing parameter μ , and ξ_2 is the phase of the SU(2) gaugino mass m_2 . The chargino contribution is given by [61]

$$a_\mu^{\chi^+} = \frac{m_\mu \alpha_{EM}}{4\pi \sin^2 \theta_W} \sum_{i=1}^2 \frac{1}{m_{\chi_i^+}} \text{Re}(\kappa_\mu U_{i2}^* V_{i1}^*) F_3 \left(\frac{m_\nu^2}{m_{\chi_i^+}^2} \right) + \frac{m_\mu^2 \alpha_{EM}}{24\pi \sin^2 \theta_W} \sum_{i=1}^2 \frac{1}{m_{\chi_i^+}^2} (|\kappa_\mu U_{i2}^*|^2 + |V_{i1}|^2) F_4 \left(\frac{m_\nu^2}{m_{\chi_i^+}^2} \right), \quad (\text{S4})$$

where the form factors are given by

$$F_3(x) = \frac{1}{(x-1)^3} (3x^2 - 4x + 1 - 2x^2 \ln x),$$

$$F_4(x) = \frac{1}{(x-1)^4} (2x^3 + 3x^2 - 6x + 1 - 6x^2 \ln x). \quad (\text{S5})$$

In Eq. (S4), U and V are defined so that $U^* M_C V^{-1} = \text{diag}(m_{\chi_1^+}, m_{\chi_2^+})$, where U and V are unitary matrices, and where $\kappa_\mu = m_\mu / \sqrt{2} M_W \cos\beta$. The phases enter via U, V and through the chargino masses. We note that the phase dependence of the chargino contribution to a_μ arises entirely from the combination $\theta_\mu + \xi_2$. The neutralino contribution, however, has additional phase dependence from ξ_1 , the phase of m_1 , and from α_{A_0} , the phase of A_0 . In Fig. S4 we show the sensitivity of Δa_μ^{FB} to CP phases ξ_1 and ξ_2 .

The top panels of Fig. S4 show the excluded regions (shaded) in the ξ_1 - ξ_2 plane due to the Δa_μ^{FB} constraint for two points chosen from the large set of points obtained from the scan. The contours shown in the allowed regions correspond to Δa_μ consistent with the combined Brookhaven and Fermilab results. Of course, the region allowed by Δa_μ^{FB} is still subject to the EDM constraints. However, the EDM allowed region must lie in the white area to satisfy the Δa_μ^{FB} constraint. The lower panel shows the sensitivity of Δa_μ to the CP phase ξ_2 with a range of values consistent with the recent $(g-2)_\mu$ experiment.

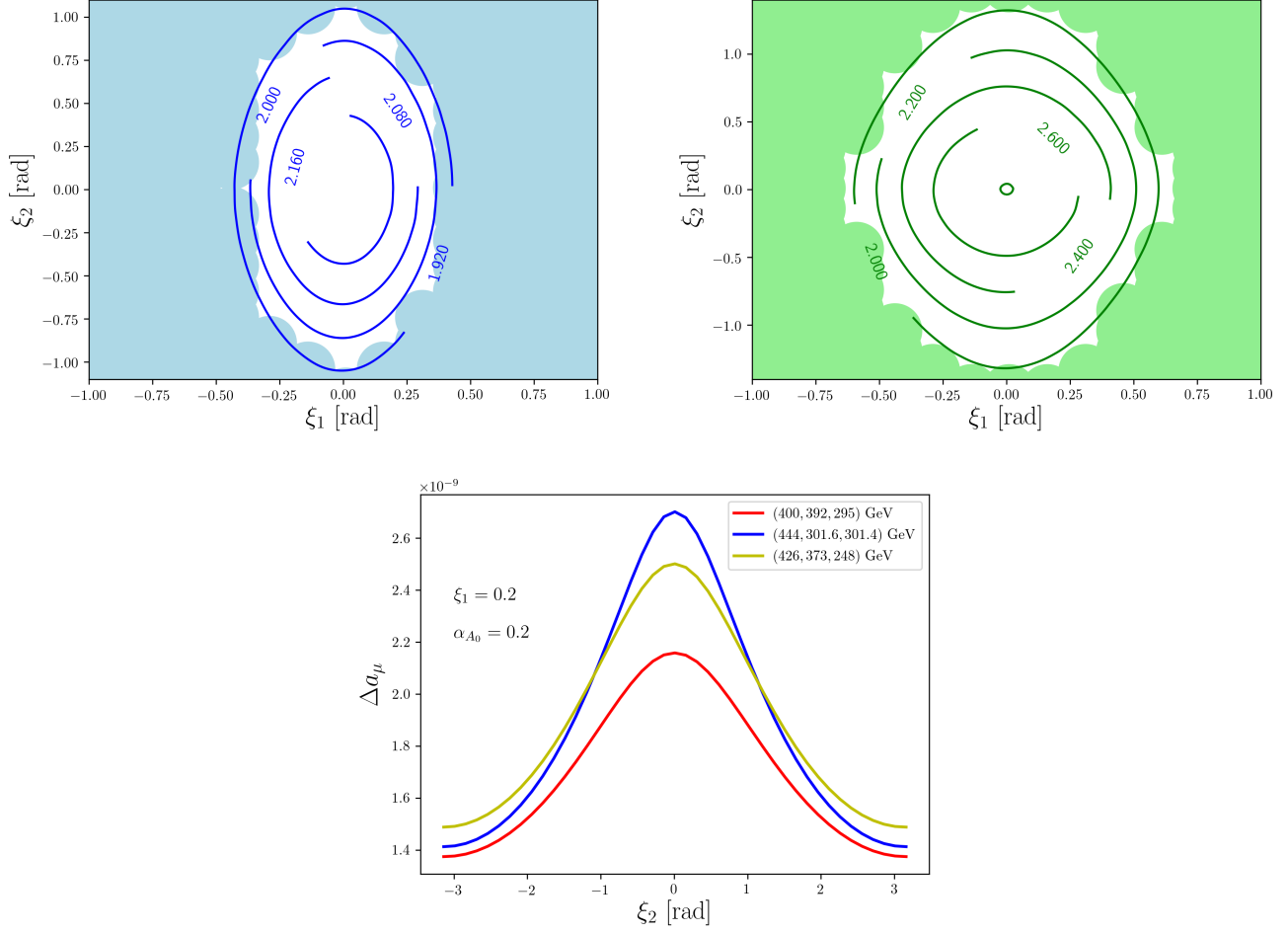


FIG. S4: Top panels: Exclusion plots in the CP phases ξ_1 and ξ_2 arising from the Δa_μ^{FB} constraint. The contours correspond to $\Delta a_\mu \times 10^9$ consistent with the combined experimental result on $g - 2$. Bottom panel: Variation of a_μ^{SUSY} with the phase ξ_2 . In all plots, $\alpha_{A_0} = 0.2$ rad. The masses of the light particles in the loops are in this order $(\tilde{\mu}, \tilde{\chi}_1^\pm, \tilde{\chi}_1^0)$: (400, 392, 1, 391.7) GeV for the top left panel and (445, 301.6, 301.4) GeV for the top right panel and shown in the legend for the bottom panel.